Received: 31 October 2023 | Revised: 20 December 2023 | Accepted: 30 December 2023

DOI: 10.1111/cas.16067

ORIGINAL ARTICLE

Cancer Science WILEY

Circular RNA circWNK1 inhibits the progression of gastric cancer via regulating the miR-21-3p/SMAD7 axis

Ting Dai[1] | Shengkui Qiu[2] | Xuesong Gao[2] | Chengjin Zhao[1] | Zhenming Ge[1] | Yanmei Yang[1] | Chong Tang[2,3] | Shichun Feng[2]

[1]Department of Gastroenterology, Nantong First People's Hospital, Affiliated Hospital 2 of Nantong University, Nantong, China

[2]Department of General Surgery, Nantong First People's Hospital, Affiliated Hospital 2 of Nantong University, Nantong, China

[3]Nantong Clinical Medical College, Kangda College of Nanjing Medical University, Nantong, China

Correspondence
Shichun Feng and Chong Tang, Department of General Surgery, Nantong First People's Hospital, Nantong 226001, Jiangsu Province, China.
Email: fsc2200@126.com and 15051273108@163.com

Funding information
Science and Technology Projects of Nantong City, Grant/Award Number: MS2021032, MS22022003 and JC2020057; Medical Research Projects of Jiangsu Provincial Health Commission, Grant/Award Number: H2019049 and Z2020079; Kangda College of Nanjing Medical University Scientific Research Development Fund, Grant/Award Number: KD2021KYJJZD085; National Natural Science Foundation of China, Grant/Award Number: 82303463; Medical Research Projects of Nantong City Health Commission, Grant/Award Number: MS2022018 and MB2021020

Abstract

Gastric cancer (GC) is a highly aggressive malignancy with limited treatment options for advanced-stage patients. Recent studies have highlighted the role of circular RNA (circRNA) as a novel regulator of cancer progression in various malignancies. However, the underlying mechanisms by which circRNA contributes to the development and progression of GC remain poorly understood. In this study, we utilized microarrays and real-time quantitative polymerase chain reaction (qRT-PCR) to identify and validate a downregulated circRNA, hsa_circ_0003251 (referred to as circWNK1), in paired GC and normal tissues. Through a series of in vitro and in vivo gain-of-function and loss-of-function assays, we demonstrated that circWNK1 exerts inhibitory effects on the proliferation, migration, invasion, and epithelial–mesenchymal transition (EMT) of GC cells. Additionally, we discovered that circWNK1 acts as a competitive endogenous RNA (ceRNA) for SMAD7 by sequestering miR-21-3p. Our findings were supported by comprehensive biological information analysis, as well as RNA pull-down, luciferase reporter gene, and western blot assays. Notably, the downregulation of circWNK1 in GC cells resulted in reduced SMAD7 expression, subsequently activating the TGF-β signaling pathway. Collectively, our study reveals that circWNK1 functions as a tumor suppressor in GC by regulating the miR-21-3p/SMAD7-mediated TGF-β signaling pathway. Furthermore, circWNK1 holds promise as a potential biomarker for the diagnosis and treatment of GC.

KEYWORDS
circWNK1, gastric cancer, miR-21-3p, SMAD7, TGF-β signaling pathway

Abbreviations: ceRNA, competitive endogenous RNA; circRNA, circular RNA; EMT, epithelial–mesenchymal transition; GC, gastric cancer; miRNA, micro RNA; MREs, miRNA response elements; ncRNA, noncoding RNAs; OS, overall survival; qRT-PCR, real-time quantitative polymerase chain reaction; SMAD, the small mother against decapentaplegic protein family; SOM, self-organizing map analysis; TCGA, The Cancer Genome Atlas; TGF-β, transforming growth factor β; TGFβ-R1, type 1 TGFβ receptor.

Ting Dai, Shengkui Qiu and Xuesong Gao contributed equally to this work.

1 | INTRODUCTION

Gastric cancer remains a significant health burden worldwide, with ~1 million new cases and 769,000 cancer-related deaths reported annually.[1,2] The pathogenic mechanisms driving GC initiation, growth, progression, and metastasis are diverse and complex, involving genetic mutations, epigenetic alterations, and dysregulated molecular signaling pathways.[3] Elucidating these underlying molecular mechanisms is critical for identifying effective biomarkers and developing therapeutic strategies targeting tumor-specific behaviors. Further research into the molecular regulation of GC is needed to enhance our knowledge and improve patient outcomes.

Since the discovery of two functional noncoding RNAs, lineage defective 4 (lin-4)[4] and lethal 7 (let-7),[5] the notion that noncoding RNAs are conserved, active molecules essential to biological processes has gained acceptance.[6] Circular RNAs are conserved single-stranded noncoding RNA produced through back splicing of exon or intron sequences during precursor mRNA transcription.[7] The distinctive circular structure of circRNAs confers resistance to 3′–5′ ribonuclease degradation.[8] Moreover, the regulatory functions of circRNAs are being extensively investigated, particularly their role as ceRNAs.[9–11] As ceRNAs, circRNAs and mRNAs sharing common MREs can competitively bind miRNAs, thereby attenuating miRNA's inhibitory effect on target mRNAs. For instance, circOSBPL10 prevents Wnt2 degradation by sequestering miR-136-5p,[12] and circNR3C1 acts as a ceRNA for cyclin D1 by sponging miR-27a-3p.[13] Our team profiled cancer-related circRNA expression in 24 pairs of GC and adjacent normal tissues in a previous study by ceRNA chip sequencing.[14] We constructed a GC circRNA regulatory network using SOM analysis and validated the network and molecular mechanisms of an upregulated circRNA, circTHBS1. However, downregulated circRNAs were not further investigated. Therefore, this study examines the role and potential mechanisms of the significantly downregulated circWNK1 in GC progression.

The TGF-β signaling pathway is critical in cellular activity. Dysregulation of this pathway has been shown to promote tumorigenesis and progression by facilitating cancer cell growth, invasion, immune evasion, and metastasis.[15–17] The SMAD family of proteins are pivotal mediators of various cellular signaling pathways. SMAD7 is an inhibitory protein that negatively regulates the TGF-β pathway by suppressing the phosphorylation of receptor-regulated SMAD proteins.[18,19] In the cytoplasm, SMAD7 competes with SMAD2/3 for binding to the type 1 TGFβ-R1, thereby blocking signal transduction by inhibiting the phosphorylation of SMAD2/3.[20] In the nucleus, SMAD7 disrupts the interaction between the SMAD2/3/4 complex and DNA.[21] Recent studies have shown that noncoding RNAs, including miRNAs and circRNAs, contribute to cancer progression by regulating SMAD7 and modulating TGF-β signaling.[22–25] However, the mechanisms underlying abnormal SMAD7 expression and its role in GC progression remain poorly understood.

This study identified a novel circular RNA, circWNK1, significantly downregulated in GC cells and tissues. Functional studies demonstrate that overexpression of circWNK1 inhibits proliferation, migration, invasion, and EMT of GC cells. Mechanistically, circWNK1 promotes SMAD7 expression and inhibits TGF-β signaling by functioning as a sponge for miR-21-3p. Our findings suggest circWNK1 may represent a novel biomarker and promising therapeutic target for GC.

2 | MATERIALS AND METHODS

2.1 | Patient samples

This study utilized formalin-fixed paraffin-embedded surgical specimens from 72 pairs of GC tissues and matched adjacent non-tumor tissues. These specimens were collected between January 2016 and January 2019 at Nantong First People's Hospital as part of routine clinical practice. All patients enrolled in this study were treatment-naïve and showed no signs of other malignancies. Patient information, including gender, age, tumor size, location, pathological differentiation, and regional or distant metastasis, was collected and evaluated. This study was conducted per the Helsinki Declaration (2013) and approved by the Ethics Committee of the Nantong First People's Hospital (No. 2022KT256).

2.2 | Statistical analysis

All cell culture experiments were performed in triplicate, and animal studies utilized six mice per group. The data were averaged across replicates or mice for statistical analyses using SPSS 26.0 (IBM, USA) and GraphPad Prism 8. Student's *t*-test evaluated the differences between the two groups. One-way ANOVA was used for comparisons of multiple groups. Pearson's correlation coefficient assessed the correlation between miR-21-3p and circWNK1 levels. The Kaplan–Meier method and log-rank test were used for survival analyses. Quantitative data are presented as mean ± standard deviation. p-values <0.05 were considered statistically significant.

2.3 | Supplementary methods

The methods of cell culture, oligonucleotide transfection, vector transfection, qRT-PCR, RNase R treatment, actinomycin D treatment, agarose gel electrophoresis, western blot, H&E staining, immunohistochemistry (IHC), RNA FISH, biotinylated circRNA pull-down assay, luciferase reporter assay, cell proliferation assays, transwell invasion, and migration assays, scratch wound healing assay, xenograft nude mouse model, the sequence of PCR primers, siRNAs, mimics, and inhibitors (Table S1), as well as the details of antibodies used in the present study (Table S2), are available in the Supplementary Materials.

3 | RESULTS

3.1 | circWNK1 is downregulated in GC cells and tissues

In a previous investigation,[14] we identified a set of circRNA–mRNA networks with potential regulatory functions using a ceRNA microarray and SOM analysis on 24 pairs of GC tissues and adjacent nontumor tissues. After SOM analysis, the top three most upregulated and top three most downregulated circRNAs were selected for validation by qRT-PCR in tissues. The most upregulated circTHBS1 was then chosen for functional and mechanistic studies. However, the downregulated circRNAs that were validated were not further investigated. Therefore, we selected the downregulated hsa_circ_0003251 (circWNK1) for further characterization. Our ceRNA microarray data showed that circWNK1 expression was significantly downregulated in GC tissues (Figure 1A–C), confirmed by qRT-PCR analysis on 72 pairs of GC tissues and normal tissues (Figure 1D,E). Additionally, compared with normal gastric mucosa cells (GES-1), circWNK1 expression was significantly lower in AGS, HGC-27, MKN-28, MKN-45, and NCI-N87 cells (Figure 1F). By analyzing qRT-PCR data from 72 GC and adjacent normal tissues, we generated a ROC curve for circWNK1. The AUC was 0.714 (Figure S1A), suggesting that circWNK1 may be a biomarker for GC diagnosis. We then analyzed the correlation between circWNK1 expression in GC tissues and clinicopathological parameters of patients (Table 1). circWNK1 expression in the T3–T4 tumor stage was significantly lower than in T1–T2 stage tumors regarding the infiltration depth (Figure 1G). Furthermore, analysis based on TNM staging showed that circWNK1 expression in stage III–IV tissues was significantly lower than in stage I–II tissues (Figure 1H). We also found that circWNK1 significantly inhibited GC cell malignant differentiation, evidenced by the correlation analysis between circWNK1 expression and histological grade (Figure 1I). Importantly, patients with low circWNK1 expression had a significantly worse 3-year OS than those with high expression (Figure 1J). These findings suggest that the downregulation of circWNK1 may be involved in GC pathogenesis.

3.2 | Molecular characteristics of circWNK1 in GC

The characteristic covalently closed-loop structure of circRNA is formed by the reverse joining of the 5′- and 3′-ends of exons or introns during the transcription process. In this study, we identified circWNK1 by aligning ceRNA microarray sequencing data with the circBase database, revealing that circWNK1 is derived from the WNK1 gene locus (chr12: 1003727–1006847) and composed of exons 21, 22, and 23 (Figure 2A). Subsequently, we extracted RNA from HGC-27 cells and confirmed the head-to-tail splicing of circWNK1 by Sanger sequencing. Furthermore, we successfully amplified products from AGS and HGC-27 cell cDNA using divergent primers, validating the circular structure of circWNK1 (Figure 2B). To determine the subcellular localization of circWNK1, we performed FISH and qRT-PCR analysis of fractionated nuclear and cytoplasmic RNA, revealing that circWNK1 is mainly located in the cytoplasm of GC cells (Figure 2C–E). We also assessed the stability of circWNK1 and found that it exhibited a longer half-life than linear WNK1 mRNA, as shown by qRT-PCR analysis at various time points after actinomycin D treatment of AGS and HGC-27 cells (Figure 2F,G). Moreover, RNase R digestion experiments further demonstrated the superior resistance of circWNK1 to ribonuclease cleavage (Figure 2H).

3.3 | circWNK1 inhibits proliferation, migration, invasion, and EMT in GC cells

To elucidate the biological role of circWNK1, we first constructed a circWNK1 overexpression plasmid and specific small interfering RNAs (si-circWNK1#1/2/3; Figure S1B), then verified their transfection efficiency in AGS and HGC-27 cells. Notably, qRT-PCR validation showed that the circWNK1 overexpression plasmid and si-circWNK1#1/2 significantly increased and decreased circWNK1 expression in GC cells, respectively, without affecting the expression of WNK1 mRNA (Figure 3A,B). Subsequently, we conducted CCK-8 proliferation assays and observed that circWNK1 overexpression in AGS cells inhibited cell proliferation, while circWNK1 knockdown in HGC-27 cells markedly accelerated proliferation (Figure 3C,D). Moreover, the suppressive effect of circWNK1 on proliferation was also detected through EdU and colony formation assays (Figure 3E–G and Figure S1C). Subsequently, we explored the impact of circWNK1 on GC cell migration and invasion using transwell chambers with or without Matrigel coating. The results indicated that transfecting AGS cells with the circWNK1 overexpression plasmid strikingly inhibited cell migration and invasion. In contrast, transfecting HGC-27 cells with si-circWNK1#2 markedly promoted these processes (Figure 3H,I). Similar results were observed in scratch assays, where overexpression and knockdown of circWNK1 inhibited the migration ability of AGS cells and promoted that of HGC-27 cells (Figure S1D,E). Additionally, we examined the expression of EMT marker proteins in transfected cells using immunofluorescence and western blotting. Overexpressing circWNK1 led to a significant increase in the epithelial marker E-cadherin and a significant decrease in the mesenchymal marker N-cadherin, implying that circWNK1 suppresses EMT in GC cells (Figure 3J–L).

3.4 | circWNK1 serves as an miRNA sponge for miR-21-3p

To investigate whether circWNK1 could function as a competing endogenous RNA (ceRNA), we utilized the online databases miRanda, TargetScan, and RNAhybrid to predict potential circWNK1-targeting miRNAs. We then intersected these prediction results with miRNAs shown to be highly expressed in GC in TCGA database, identifying seven candidate miRNAs (Figure 4A). To validate the interaction between circWNK1 and these miRNAs, we performed RNA pull-down

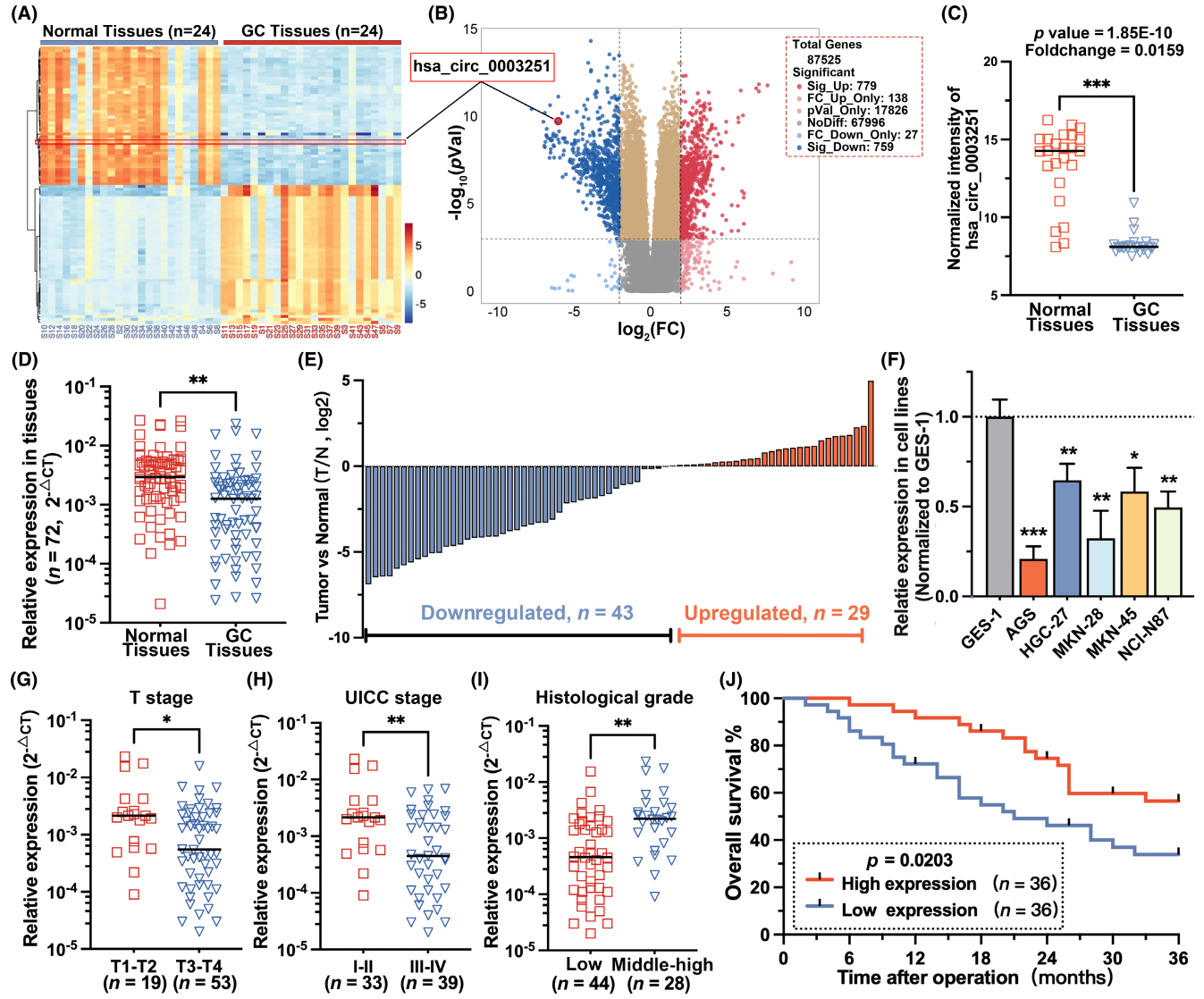

FIGURE 1 circWNK1 downregulation in GC cells and tissues. (A) Heatmap of the top 100 differentially expressed circRNAs in microarray sequencing data. (B) Volcano plot based on ceRNA microarray sequencing results, highlighting significant downregulation of hsa_circ_0003251. (C) Microarray data showing significant downregulation of hsa_circ_0003251 in GC tissues compared with normal tissues. (D) qRT-PCR confirming downregulation of hsa_circ_0003251 in GC tissues. (E) Fold change in hsa_circ_0003251 expression between paired GC tissues and paraneoplastic normal tissues. (F) Expression of circWNK1 was significantly downregulated in GC cells compared with normal gastric mucosa cells. (G) Association between circWNK1 expression and T stage evaluated using qRT-PCR. (H) Association between circWNK1 expression and UICC tumor TNM staging evaluated. (I) Association between circWNK1 expression and tumor histological grade evaluated. (J) Kaplan–Meier analysis showing worse overall survival for GC patients with low circWNK1 expression. $^{*}p<0.05$, $^{**}p<0.01$, $^{***}p<0.001$.

assays using a biotin-labeled probe specific for circWNK1. This circWNK1-specific probe enriched more circWNK1 from lysates of AGS and HGC-27 cells than a control oligo probe (Figure 4B). We then quantified the enrichment of the candidate miRNAs in the pull-down using qRT-PCR. In AGS cells, miR-21-3p, miR-301b-5p, miR-3619-5p, and miR-551a were significantly enriched by the circWNK1 probe compared with the other candidates (Figure 4C). Similarly, in HGC-27 cells, the circWNK1 probe enriched miR-21-3p, miR-301b-5p, miR-3200-3p, and miR-551a more than other predicted targets (Figure 4D). We selected three enriched miRNAs based on these pull-down results for further target validation. We constructed a luciferase reporter containing the circWNK1 sequence downstream of luciferase (LUC-circWNK1) and co-transfected it with different miRNA mimics into HEK293T cells. Only transfection with miR-21-3p mimics significantly reduced the luciferase activity (Figure 4E). We further generated a reporter with mutated miR-21-3p binding sites in the circWNK1 sequence (Figure 4F) and found no decrease in luciferase activity in cells co-transfected with miR-21-3p mimics (Figure 4G,H). These findings collectively indicated that miR-21-3p, but not other miRNAs, directly bound to circWNK1. Furthermore, the co-localization of Cy3-labeled circWNK1 and FAM-labeled miR-21-3p in the cytoplasm, as demonstrated by FISH, offers further

TABLE 1 Associations between circWNK1 expression and clinicopathological characteristics in GC patients ($n = 72$).

Parameters	Category	No.	Expression of circWNK1		*p*-value
			High (36)	Low (36)	
Age	<60	26	11	15	0.3264
	≥60	46	25	21	
Gender	Male	46	22	24	0.6236
	Female	26	14	12	
Tumor site	Cardiac	32	14	18	0.3428
	Noncardiac	40	22	18	
T stage	T1–T2	19	14	5	0.0161*
	T3–T4	53	22	31	
N stage	Negative	26	16	10	0.1410
	Positive	46	20	26	
UICC stage	I–II	33	21	12	0.0333*
	III–IV	39	15	24	
Differentiation	Well moderately	28	19	9	0.0156*
	Poorly signet	44	17	27	
Vessel invasion	Yes	55	28	27	0.7814
	No	17	8	9	

Note: Chi-squared test, $^*p < 0.05$.

substantiation of their direct interaction (Figure 3I). In summary, we confirmed that circWNK1 acts as a sponge for miR-21-3p in the cytoplasm.

3.5 | miR-21-3p reverses the tumor-suppressive effect of circWNK1 in GC cells

To investigate the role of miR-21-3p in GC, we analyzed data from TCGA database and found that miR-21-3p expression was significantly upregulated in GC tissues compared with normal tissues (Figure 5A). Moreover, miR-21-3p expression escalated with the advancing tumor stage (Figure 5B). Consistent with this, qRT-PCR showed that miR-21-3p was markedly increased in GC cells and tissues compared with normal gastric mucosal cells (GES-1) and normal gastric tissues (Figure 5C,D), implying an oncogenic role in GC. Prior to investigating whether miR-21-3p is involved in the regulatory effect of circWNK1 on GC cells, we examined the impact of miR-21-3p on circWNK1 expression. It was observed that transfection of miR-21-3p mimics and inhibitors did not affect the expression of circWNK1 in AGS and HGC-27 cells (Figure S1F,G). Furthermore, there was no apparent correlation between the expression of circWNK1 and miR-21-3p in GC tissues (Figure S1H), suggesting that circWNK1 might function as a "molecular sponge." Then, EdU assays showed that circWNK1 overexpression substantially suppressed AGS cell proliferation, which was dramatically reversed by co-transfection with miR-21-3p mimics (Figure 5E). Conversely, circWNK1 knockdown in HGC-27 cells increased proliferation, while co-transfection with miR-21-3p inhibitors mitigated this (Figure 5H). Moreover, miR-21-3p mimics reversed the inhibitory effects of circWNK1 overexpression on AGS cell migration and invasion (Figure 5F). In addition, miR-21-3p inhibitors alleviated the promigratory and proinvasive effects induced by circWNK1 knockdown in HGC-27 cells (Figure 5I). Subsequently, immunofluorescence and western blotting revealed that circWNK1 overexpression in AGS cells increased E-cadherin and decreased N-cadherin expression, and the effects were weakened by miR-21-3p mimics (Figure 5K,L). In HGC-27 cells, circWNK1 knockdown had opposite impacts on E-cadherin and N-cadherin, reversed by miR-21-3p inhibitors (Figure 5M,N). These findings suggest that circWNK1 inhibits GC cell proliferation, migration, invasion, and EMT by sequestering miR-21-3p.

3.6 | SMAD7 is the target gene of miR-21-3p

To identify the target genes of miR-21-3p, we utilized four databases—miRDB, TarBase, TargetScan, and miRmap—and identified 39 overlapping target genes (Figure 6A). Given the negative regulatory relationship between miRNAs and their target genes and the oncogenic role of miR-21-3p in GC that we validated, we selected four genes for further validation. These four genes—ALCAM, DAB2IP, SMAD7, and TAP1—have reported tumor-suppressive functions from the 39 candidates. qRT-PCR results showed that only SMAD7 expression decreased and increased correspondingly in AGS and HGC-27 cells transfected with miR-21-3p mimics and inhibitors, suggesting that SMAD7 may be a direct target of miR-21-3p (Figure 6B,C). Moreover, SMAD7 expression was significantly decreased in GC tissues compared with normal tissues (Figure 6D). We conducted a linear analysis using TCGA database data and our

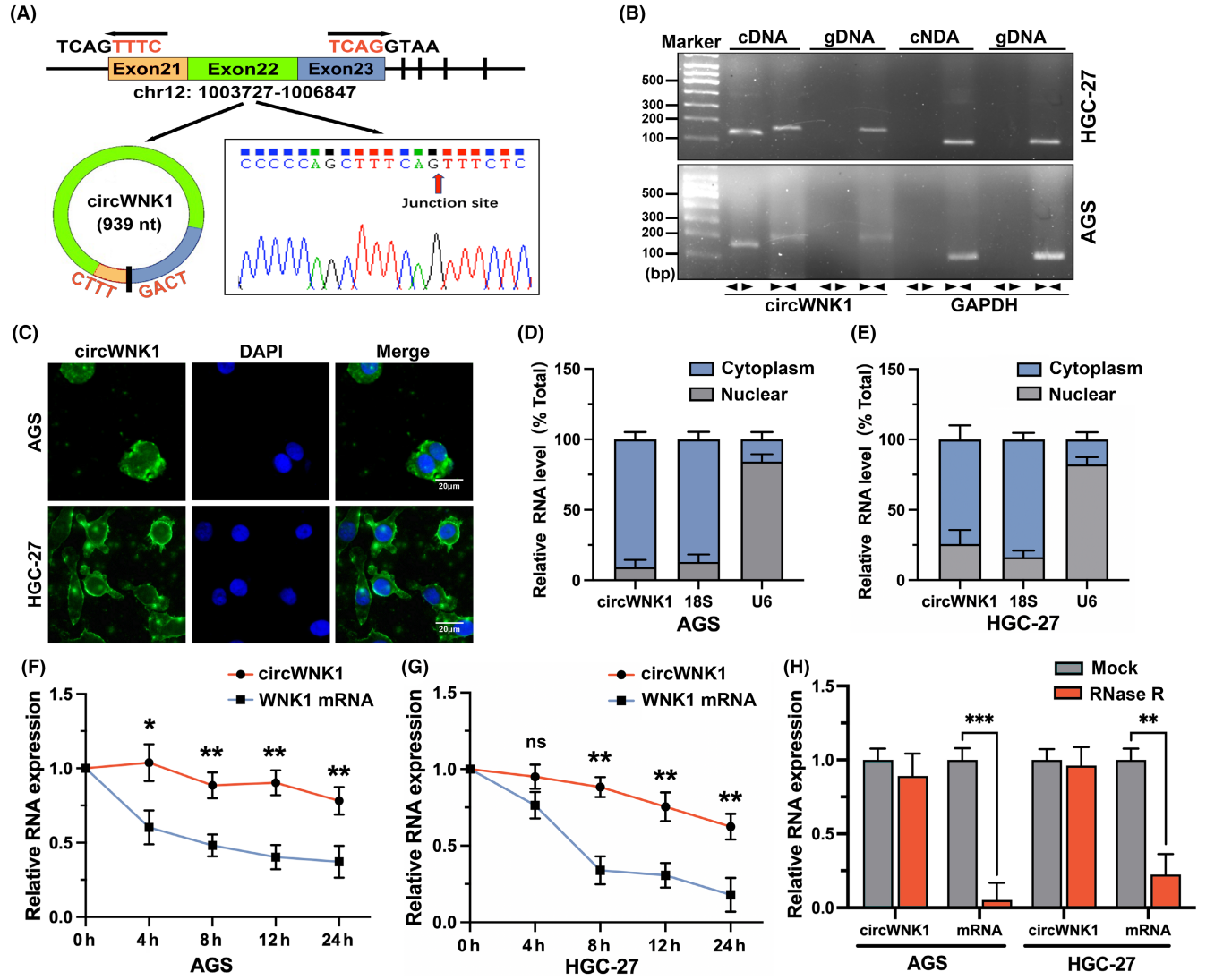

FIGURE 2 Molecular characteristics of circWNK1 in GC. (A) circWNK1 derived from exons 21–23 of the *WNK1* gene, confirmed by Sanger sequencing. (B) Successful amplification of cDNA using divergent primers in AGS and HGC-27 cells shown by northern blotting. (C) FISH indicating cytoplasmic localization of circWNK1 in AGS and HGC-27 cells. Scale bar represents 20 μm. (D, E) Enrichment of circWNK1 in the cytoplasm demonstrated by qRT-PCR of nuclear and cytoplasmic fractions. (F, G) Greater stability of circWNK1 compared with linear *WNK1* mRNA after actinomycin D treatment in AGS and HGC-27 cells. (H) Resistance of circWNK1 to exonuclease-mediated degradation shown by RNase R treatment. $^{*}p<0.05$, $^{**}p<0.01$, $^{***}p<0.001$.

center's patient qRT-PCR data and discovered a significant negative association between SMAD7 expression and miR-21-3p levels (Figure 6E and Figure S1I). Bioinformatic analysis predicted a putative 7-mer-m8 binding site with miR-21-3p in the 3′UTR of the SMAD7 transcript, and dual luciferase reporter genes were designed accordingly (Figure 6F). As shown in Figure 6G,H, miR-21-3p mimics significantly reduced the luciferase activity of wild-type SMAD7 in AGS and HGC-27 cells but had no effect on mutant SMAD7, indicating that miR-21-3p can specifically bind to the 3′UTR region of SMAD7. Additionally, western blot analysis revealed that SMAD7 expression was markedly inhibited in AGS and enhanced in HGC-27 cells transfected with miR-21-3p mimics and inhibitors, respectively, versus negative control (Figure 6I).

3.7 | SMAD7 reverses the effects of circWNK1 on GC cells

We performed rescue experiments to investigate whether circWNK1 inhibited the malignant phenotype of GC cells by regulating the expression of SMAD7. As SMAD7 is an inhibitory SMAD protein that negatively regulates the TGF-β signaling pathway, we examined the expression changes of SMAD7 and other essential TGF-β pathway proteins in co-transfected GC cells by western blot. When circWNK1 was knocked down in AGS cells, the phosphorylation of Smad2, Smad3, and upregulation of P21 expression were observed. However, this activation of the TGF-β pathway was reversed by co-transfection with a SMAD7 overexpression plasmid. Conversely,

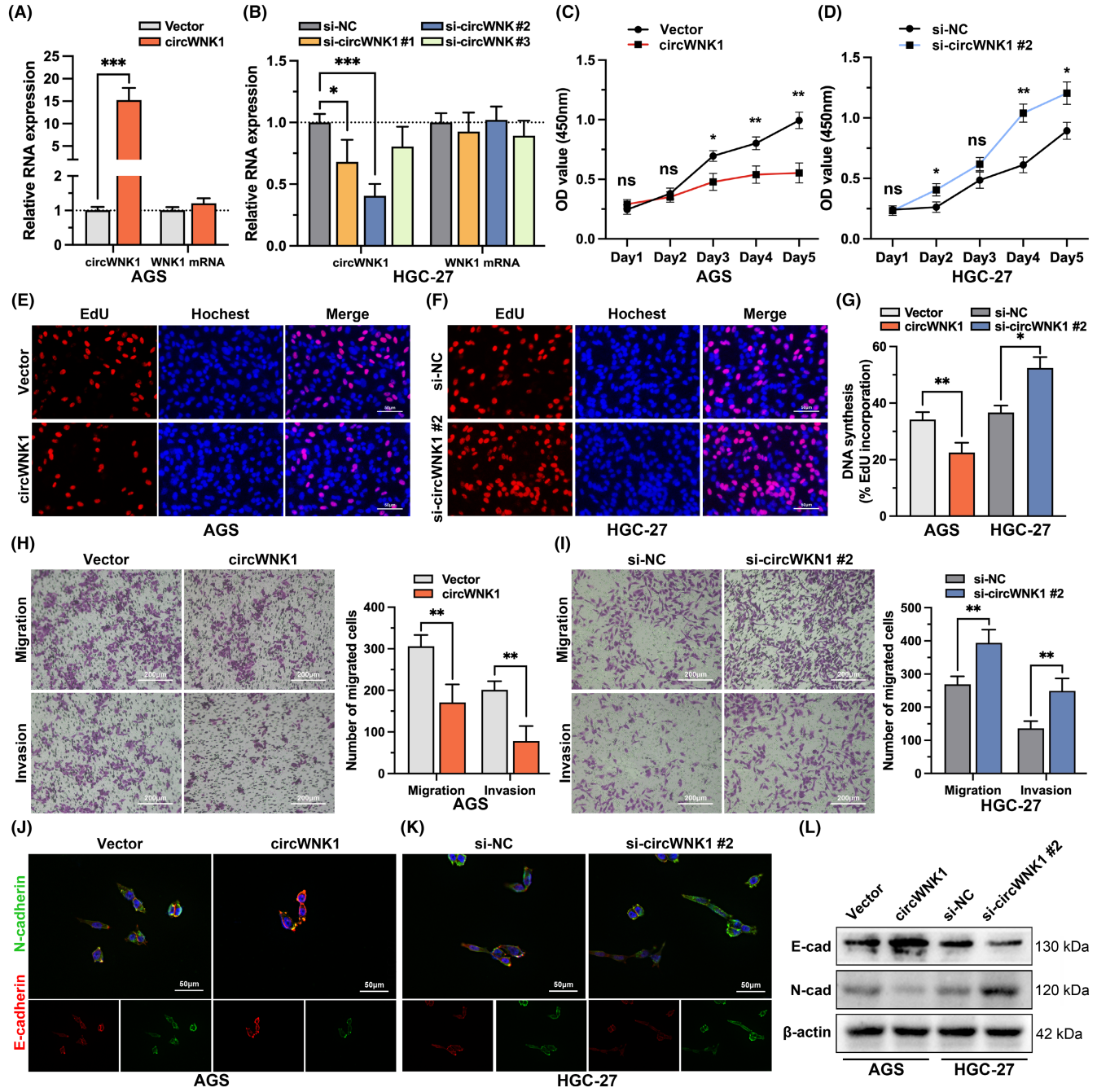

FIGURE 3 circWNK1 inhibits proliferation, migration, invasion, and EMT in GC cells. (A, B) Validation of knockdown and overexpression efficiency of circWNK1 using qRT-PCR. (C) Inhibitory effect of circWNK1 overexpression on AGS cell proliferation assessed by CCK-8 assay. (D) Effect of circWNK1 knockdown on HGC-27 cell proliferation assessed by CCK-8 assay. (E–G) EdU incorporation assays evaluating proliferation after circWNK1 overexpression in AGS cells or knockdown in HGC-27 cells. Scale bars represent 50 μm. (H, I) Investigation of circWNK1 overexpression or knockdown effects on GC cell migration and invasion using transwell assays. Scale bars represent 200 μm. (J, K) Assessment of E-cadherin and N-cadherin expression in AGS and HGC-27 cells using immunofluorescence upon circWNK1 overexpression or knockdown. Red signal: E-cadherin, green signal: N-cadherin, blue nuclei stained with DAPI. Scale bar represents 50 μm. (L) Western blot analysis examining the effects of circWNK1 overexpression or knockdown on E-cadherin and N-cadherin levels in GC cells. $^{*}p < 0.05$, $^{**}p < 0.01$, $^{***}p < 0.001$.

in HGC-27 cells, the inhibitory effect of circWNK1 overexpression on TGF-β signaling was reversed after co-transfection with siRNA targeting SMAD7 (Figure 7A). To further investigate whether circWNK1's effects on GC cell proliferation and metastasis are mediated by SMAD7, functional rescue experiments were performed. EdU assays and colony formation assays showed that the promoting and inhibiting effects on GC cell proliferation by circWNK1 knockdown and overexpression, respectively, were abolished when SMAD7 was overexpressed or knocked down (Figure 7B,C and Figure S2A,C). These results implicated SMAD7 as a critical mediator of circWNK1's

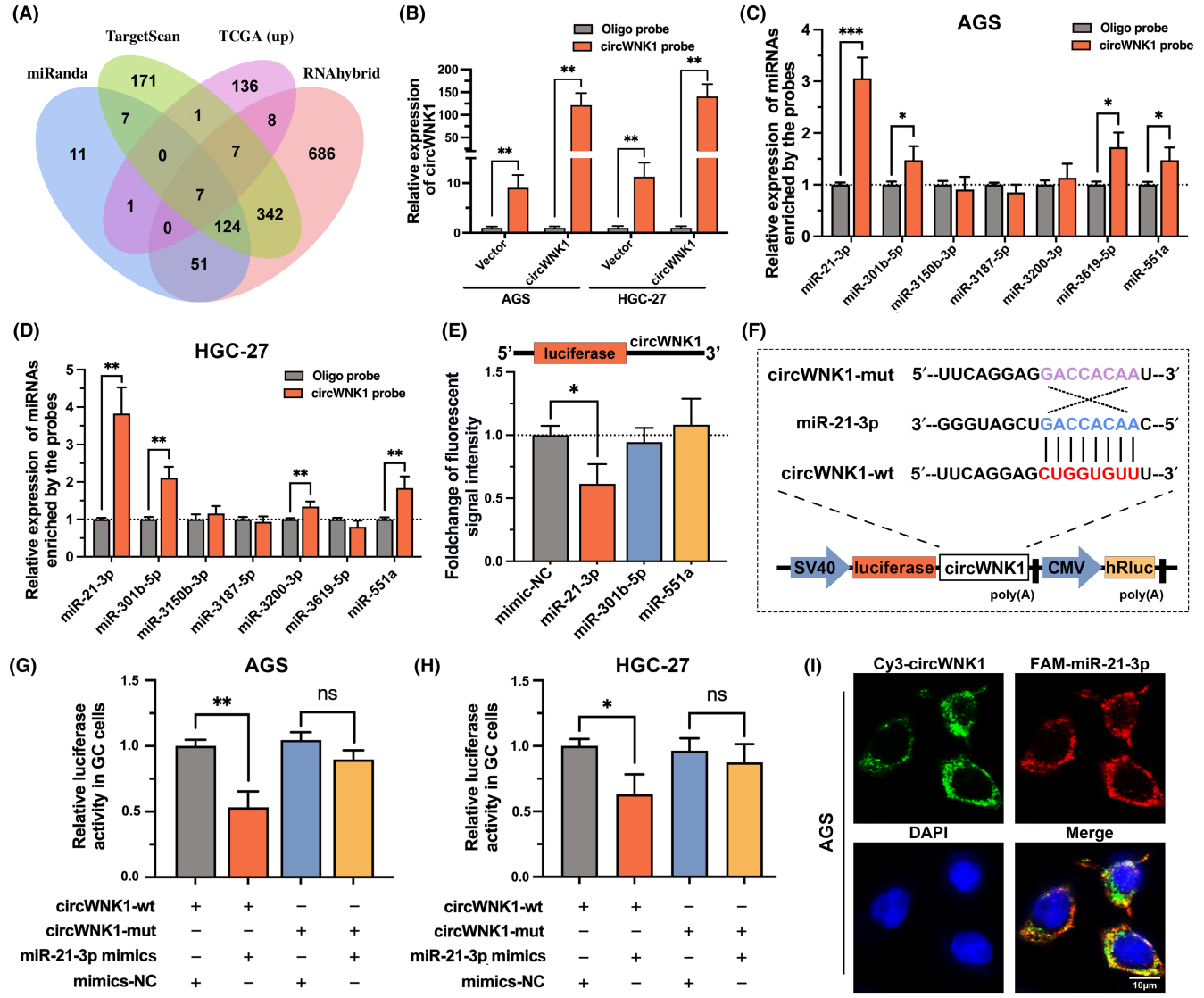

FIGURE 4 circWNK1 as an miRNA sponge for miR-21-3p. (A) Venn diagram shows predicted miRNAs targeted by circWNK1. (B) RNA pull-down assay confirms the enrichment of circWNK1 in AGS and HGC-27 cells. (C, D) qRT-PCR reveals the abundance of predicted miRNAs pulled down by circWNK1 probe. (E) Luciferase reporter assays demonstrate decreased luciferase activity for luc-circWNK1 with miR-21-3p mimics. (F) Schematic representation of putative binding sites of miR-21-3p with circWNK1. (G, H) Luciferase reporter assays validate miR-21-3p binding to wild-type or mutant circWNK1 luciferase plasmids. (I) FISH assays show the co-localization of circWNK1 and miR-21-3p in AGS cells. $^{*}p<0.05$, $^{**}p<0.01$, $^{***}p<0.001$.

regulation of cell proliferation. Similarly, increased migration and invasion of AGS cells after circWNK1 knockdown were significantly attenuated following co-transfection with SMAD7 overexpression plasmids (Figure 7D,E and Figure S2B). Overexpression of circWNK1 significantly inhibited HGC-27 cell migration and invasion, which was abrogated by si-SMAD7 co-transfection (Figure 7F,G and Figure S2D). Moreover, immunofluorescence detected expression changes of EMT-related proteins in rescue experiments. In AGS cells, knockdown of circWNK1 increased N-cadherin expression and decreased E-cadherin expression, and effects were reversed

FIGURE 5 Overexpression of miR-21-3p reverses circWNK1's inhibitory effect on GC cells. (A, B) Analysis of TCGA database reveals increased miR-21-3p expression in GC tissues and its association with advancing tumor stage. (C) qRT-PCR confirms the upregulation of miR-21-3p in GC cell lines. (D) qRT-PCR validates miR-21-3p upregulation in GC tissues. (E–G) EdU and transwell assays assess changes in proliferation, migration, and invasion of AGS cells after transfection with miR-21-3p mimics and circWNK1 overexpression plasmid. (H–J) EdU and transwell assays evaluate changes in proliferation, migration, and invasion of HGC-27 cells following transfection with the miR-21-3p inhibitor and si-circWNK1#2. (K, L) Immunofluorescence staining and western blot analysis demonstrate the effect of co-transfection on E-cadherin and N-cadherin expression in AGS cells. (M, N) Immunofluorescence staining and western blot analysis investigate the effect of co-transfection on E-cadherin and N-cadherin expression in HGC-27 cells. $^{*}p<0.05$, $^{**}p<0.01$, $^{***}p<0.001$.

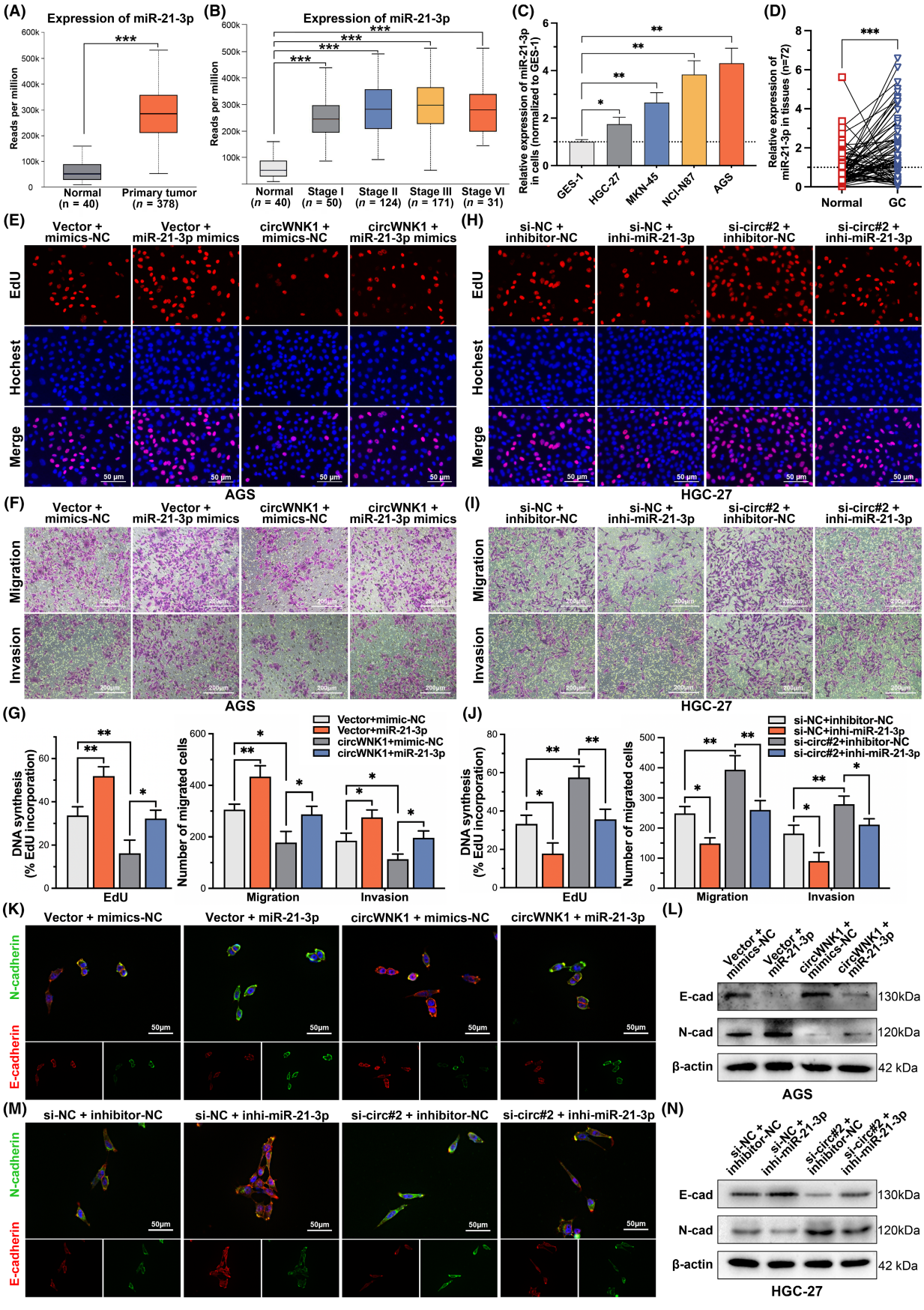
(A)
Expression of miR-21-3p
Reads per million
Normal (n = 40)
Primary tumor (n = 378)
(B)
Expression of miR-21-3p
Normal (n = 40)
Stage I (n = 50)
Stage II (n = 124)
Stage III (n = 171)
Stage VI (n = 31)
(C)
Relative expression of miR-21-3p in cells (normalized to GES-1)
GES-1
HGC-27
MKN-45
NCI-N87
AGS
(D)
Relative expression of miR-21-3p in tissues (n=72)
Normal
GC
(E)
Vector + mimics-NC
Vector + miR-21-3p mimics
circWNK1 + mimics-NC
circWNK1 + miR-21-3p mimics
EdU
Hochest
Merge
AGS
(H)
si-NC + inhibitor-NC
si-NC + inhi-miR-21-3p
si-circ#2 + inhibitor-NC
si-circ#2 + inhi-miR-21-3p
HGC-27
(F)
Migration
Invasion
(I)
(G)
DNA synthesis (% EdU incorporation)
Number of migrated cells
Vector+mimic-NC
Vector+miR-21-3p
circWNK1+mimic-NC
circWNK1+miR-21-3p
EdU
Migration
Invasion
(J)
si-NC+inhibitor-NC
si-NC+inhi-miR-21-3p
si-circ#2+inhibitor-NC
si-circ#2+inhi-miR-21-3p
(K)
Vector + mimics-NC
Vector + miR-21-3p
circWNK1 + mimics-NC
circWNK1 + miR-21-3p
N-cadherin
E-cadherin
(L)
E-cad
N-cad
β-actin
130kDa
120kDa
42 kDa
AGS
(M)
si-NC + inhibitor-NC
si-NC + inhi-miR-21-3p
si-circ#2 + inhibitor-NC
si-circ#2 + inhi-miR-21-3p
(N)
HGC-27

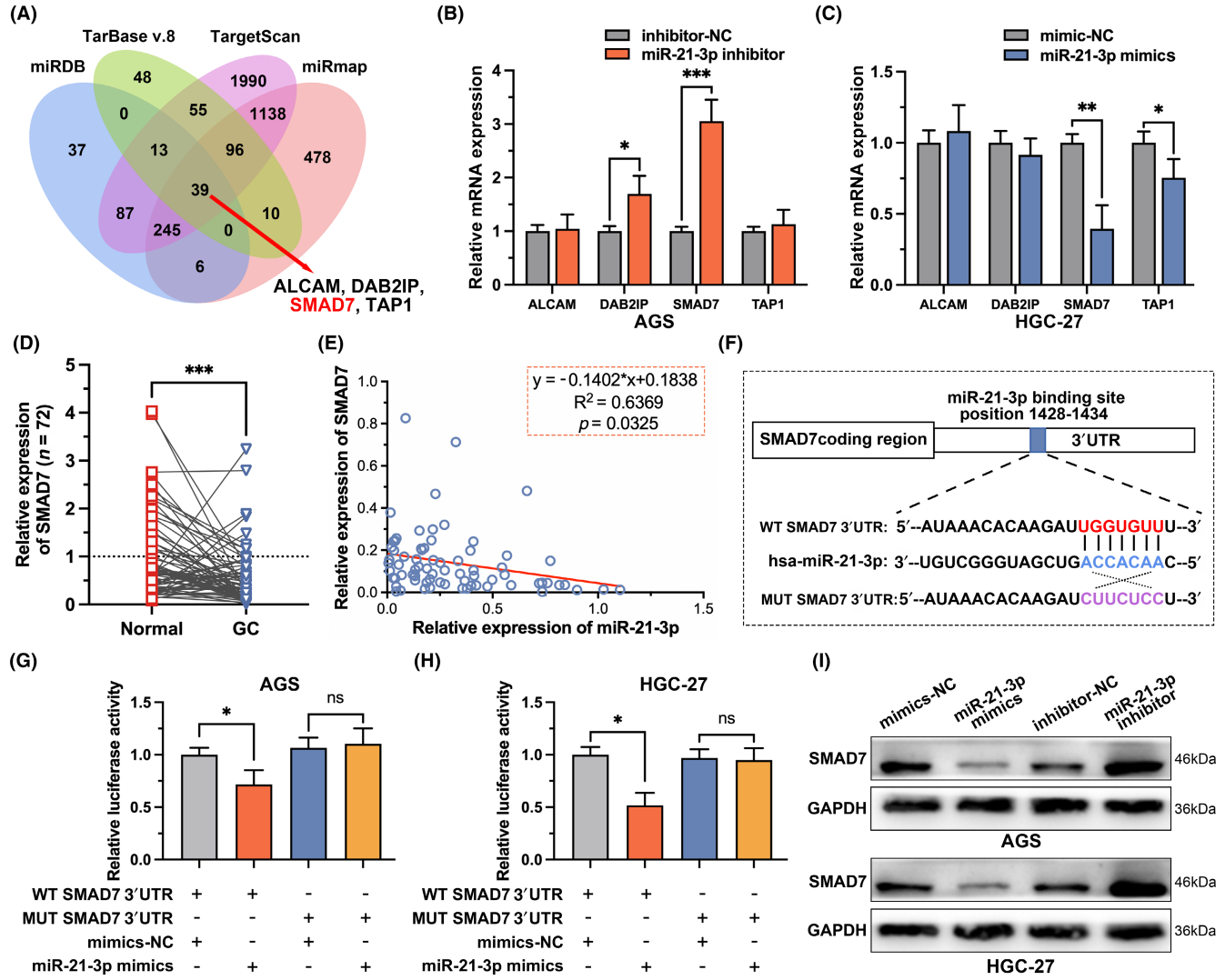

FIGURE 6 *SMAD7* as target gene of miR-21-3p. (A) Venn diagram shows common target mRNAs of miR-21-3p, highlighting four tumor suppressor genes. (B, C) qRT-PCR examines the expression of the four predicted targets in GC cells following transfection with miR-21-3p inhibitors and mimics. (D) qRT-PCR detects miR-21-3p expression in GC tissues. (E) Linear analysis shows a negative correlation between SMAD7 and miR-21-3p. (F) Putative binding site of miR-21-3p to SMAD7 and mutant sequence. (G, H) Luciferase reporter assays assess the binding of miR-21-3p to *SMAD7* 3′UTR. (I) Western blot measures SMAD7 expression after miR-21-3p inhibitors or mimics transfection. $^{*}p < 0.05$, $^{**}p < 0.01$, $^{***}p < 0.001$.

by SMAD7 overexpression (Figure 7H,I). In HGC-27 cells, the effects of circWNK1 overexpression on E-cadherin and N-cadherin were reversed by SMAD7 knockdown (Figure 7J,K). Collectively, these results indicated that circWNK1's inhibitory effects on GC cell proliferation, migration, invasion, and EMT are principally mediated through SMAD7.

3.8 | circWNK1 contributes to tumor growth and metastasis in vivo

To investigate the role of circWNK1 in tumor growth in vivo, stable circWNK1 knockdown or overexpressing GC cells were subcutaneously injected into the inguinal region of nude mice to establish a subcutaneous tumor model. Examination of tumor volume and weight revealed that the proliferation of subcutaneous tumors formed by circWNK1-overexpressing AGS cells was significantly inhibited versus control (Figure 8A,B). Conversely, the volume and weight of subcutaneous tumors formed by circWNK1 knockdown HGC-27 cells were markedly increased (Figure 8D,E). Ki-67 staining revealed that circWNK1 overexpression and knockdown in AGS and HGC-27 cells, respectively, inhibited and promoted the proliferation of subcutaneous tumors (Figure 8C,F). Furthermore, a model for lung metastasis was created by injecting fluorescence-labeled GC cells with stable circWNK1 silencing or overexpression into the tail veins of nude mice. Four weeks after injection, an in vivo imaging system was used to examine lung metastasis. Compared with the control, lung metastasis of circWNK1-overexpressing AGS cells was significantly inhibited, while circWNK1 knockdown HGC-27 cells showed enhanced metastasis (Figure 7G,H). H&E staining of mouse lungs corroborated these results

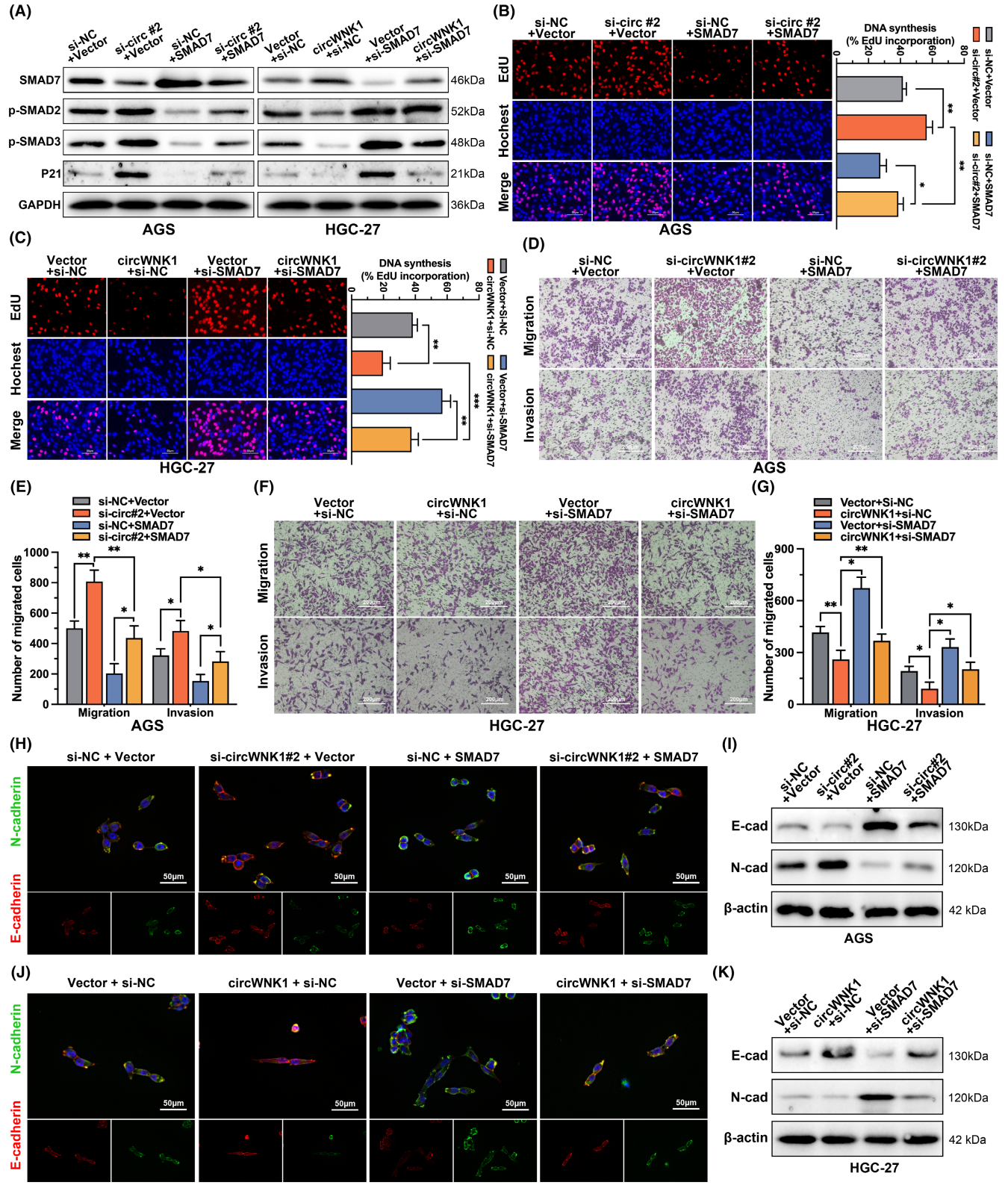

FIGURE 7 SMAD7 reverses the effects of circWNK1 on GC cells. (A) Western blot shows altered expression of key TGF-β pathway proteins in AGS and HGC-27 cells after co-transfection. (B, C) EdU assay demonstrates the reversal of circWNK1's antiproliferative effect by SMAD7. (D–G) Transwell assays show SMAD7 abolishing anti-migratory and anti-invasive effects of circWNK1. (H, I) Immunofluorescence and western blot reveal the reversal of EMT promotion induced by circWNK1 knockdown in AGS cells. (J, K) Immunofluorescence and western blot demonstrate the reversal of EMT inhibition by circWNK1 overexpression in HGC-27 cells. $^{*}p<0.05$, $^{**}p<0.01$, $^{***}p<0.001$.

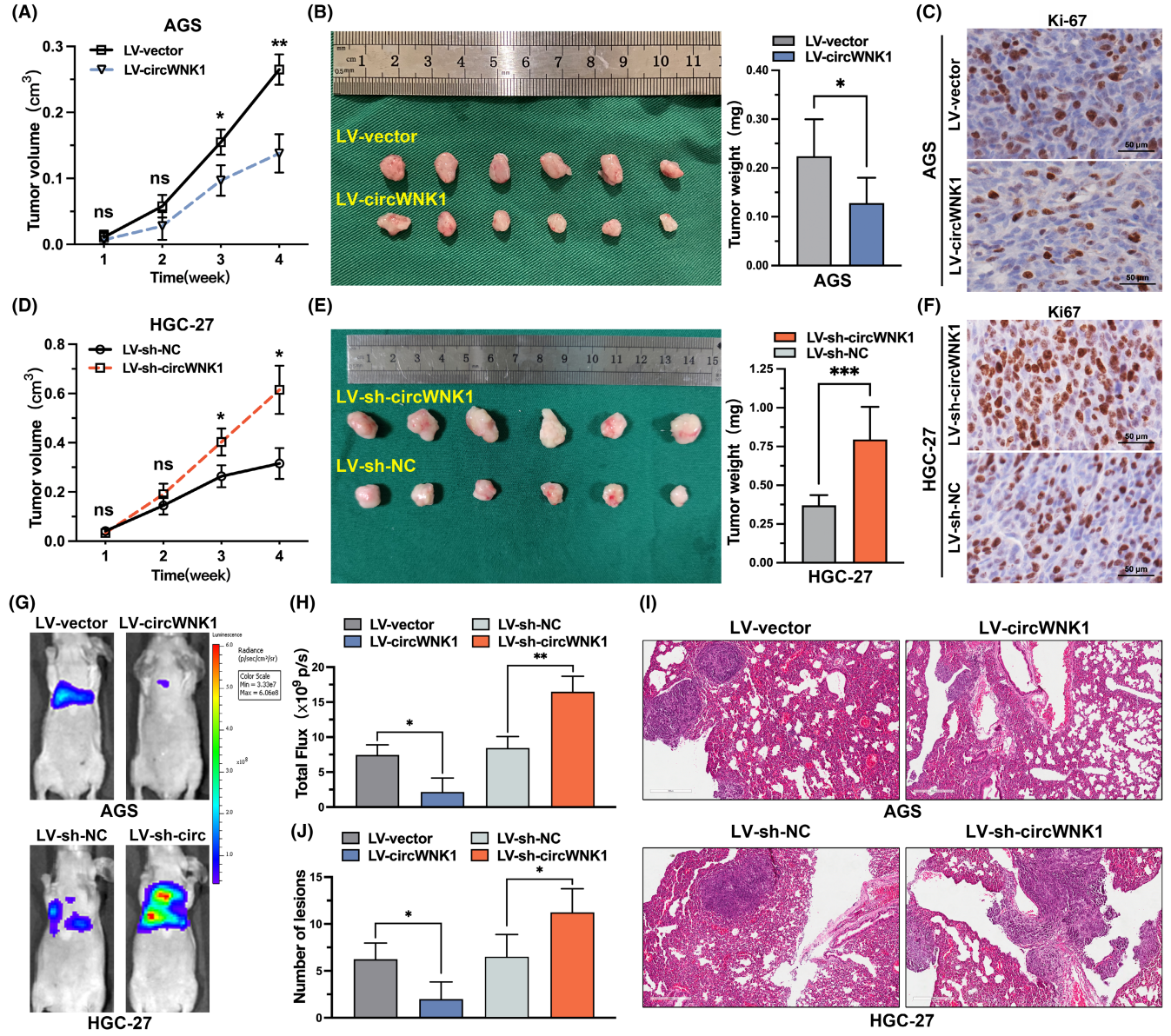

FIGURE 8 circWNK1 contributes to tumor growth and metastasis in vivo. (A and B) Stable circWNK1-overexpressing AGS cells were injected subcutaneously into nude mice. Tumor volume was measured weekly, and tumors were harvested and weighed at 4 weeks. (C) Representative Ki-67 staining of subcutaneous tumors from stable circWNK1-overexpressing AGS cells. (D and E) Stable circWNK1 knockdown HGC-27 cells injected subcutaneously into nude mice. Tumor volume was measured weekly, and tumors were harvested and weighed at 4 weeks. (F) Representative Ki-67 staining of subcutaneous tumors from stable circWNK1 knockdown HGC-27 cells. (G and H) Fluorescently-labeled stable circWNK1-overexpressing or knockdown GC cells injected into mouse tail veins. Bioluminescent imaging detected in vivo fluorescence intensity. Representative images were shown, and fluorescence intensity was statistically evaluated. (I and J) Representative H&E lung metastasis nodule images and quantification from mice with different interventions. $^{*}p < 0.05$, $^{**}p < 0.01$, $^{***}p < 0.001$.

(Figure 8I,J). These in vivo data demonstrated that circWNK1 inhibits GC cell proliferation and metastasis.

4 | DISCUSSION

It is widely recognized that the human genome contains many functional ncRNAs.[26,27] circRNAs, a newly identified class of ncRNAs, have been shown to participate in various cellular processes, especially tumor proliferation, invasion, metastasis, and therapeutic resistance.[8,28] This study identified circWNK1 as significantly downregulated in GC by analyzing previous microarray data and validating candidates by qRT-PCR. Functional assays in vitro and in vivo indicated that circWNK1 is a tumor suppressor in GC. Mechanistically, circWNK1 functions as a ceRNA that sequesters miR-21-3p, reversing its inhibitory effect on SMAD7, and consequently regulating GC cell proliferation, migration, invasion, and EMT (Figure 9).

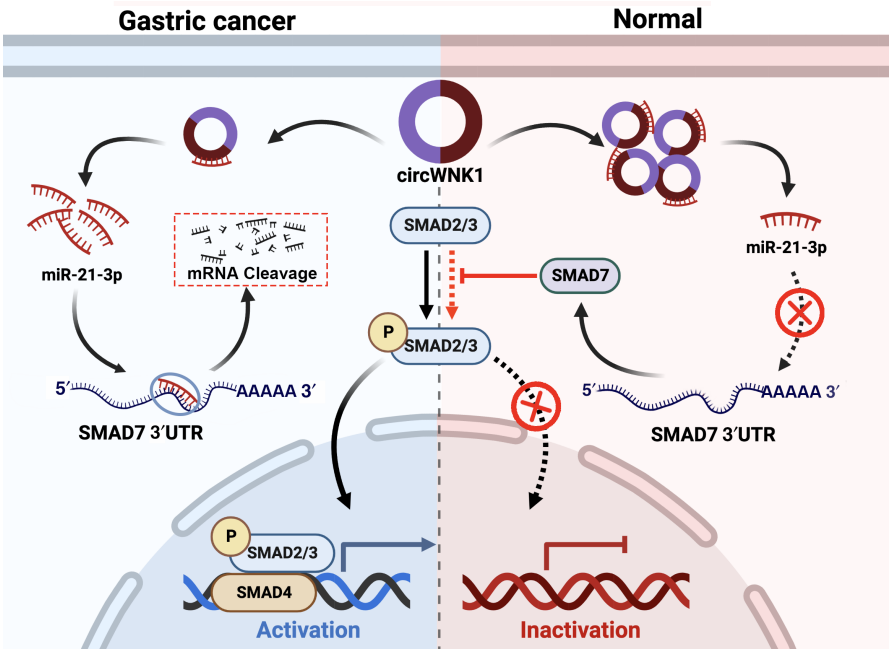

FIGURE 9 Molecular mechanism schematic diagram of circWNK1 inhibiting GC progression.

The unique covalent closed-loop structure, formed through reverse splicing, endows circRNAs with more excellent stability than linear mRNA.[29] We confirmed that circWNK1 has a longer half-life and increased resistance to RNase R versus WNK1 mRNA. Moreover, circRNAs demonstrated abundant, tissue-specific expression, conferring utility as disease biomarkers.[30] Previous studies have revealed diverse, dynamic circRNA roles in tumorigenesis,[13] immune responses,[31] and infections.[32] In this study, we found that high expression of circWNK1 was associated with better prognosis and negatively correlated with GC infiltration depth and differentiation. However, we did not assess circWNK1 in plasma, so we could not conclude that it is a liquid biopsy biomarker for GC.

circRNAs modulate intracellular activities via various mechanisms,[7,33] including acting as ceRNAs,[34] forming functional complexes through interactions with RNA-binding proteins[35] and encoding peptides or proteins.[36] Using bioinformatics analysis, we sought to illuminate the downstream mechanisms of circWNK1, identifying miR-21-3p as a critical functional target. Recent investigations have underscored the oncogenic role of miR-21-3p across a range of malignancies. Notably, in colon cancer, miRNA sequencing has indicated a considerable upregulation of miR-21-3p expression relative to normal mucosa, suggesting its significant role in colon carcinogenesis.[37] miR-21-3p has also been associated with tumor immunosuppression by binding to the 3′UTR of TAP1 and downregulating its expression.[38] Furthermore, miR-21-3p has been implicated in promoting cell proliferation and anti-apoptosis in esophageal cancer by regulating TRAF4.[39] However, the precise role of miR-21-3p in the progression of GC remains to be fully elucidated. Our research demonstrates that miR-21-3p upregulation promotes proliferation, migration, invasion, and EMT of GC cells and counteracts the tumor-suppressive effect of circWNK1 overexpression. These data support an oncogenic role of miR-21-3p in GC progression and indicates that circWNK1 operates as a molecular sponge that sequesters miR-21-3p.

miRNAs suppress target mRNA expression by binding to the 3′UTR in a sequence-specific manner.[40,41] In our research, we confirmed that miR-21-3p directly binds to the 3′UTR region of SMAD7, significantly reducing both its mRNA and protein levels. As an inhibitor protein of the TGF-β pathway, SMAD7 functions to block or attenuate signal transduction either by inducing TGF-βR1 degradation through the recruitment of SMURF2 (E3 ubiquitin ligase) or by inhibiting the phosphorylation of SMAD2 to prevent the polymerization of SMAD2 and SMAD4.[21] Dysregulation of the TGF-β family signaling pathway has been implicated in developmental abnormalities and disease, while enhanced TGF-β signaling has been linked to cancer and fibrosis.[42–44] Our study suggests that circWNK1 regulates SMAD7 expression via a ceRNA mechanism, subsequently influencing TGF-β signaling and tumor progression in GC. The TGF-β signaling pathway has been broadly studied in various epithelial cancers, including breast, lung, pancreatic, and colorectal cancers.[17,45] Our rescue experiments indicated that circWNK1 primarily activates TGF-β signaling in GC cells by acting as ceRNA for SMAD7. Although our in vivo and in vitro experiments confirmed that circWNK1 inhibits its GC progression by sponging miR-21-3p and suppressing SMAD7 expression, it remains unclear whether circWNK1 can also function as an anti-oncogene through other pathways.

In conclusion, our study highlights the crucial role of circWNK1 in suppressing tumor growth in GC through its inhibitory effects on cell proliferation, migration, invasion, and EMT. Specifically, we have identified circWNK1 as an miR-21-3p sponge, which subsequently enhances SMAD7 expression to exert its tumor-suppressive function. These significant findings provide valuable insights into the molecular mechanisms involved in GC progression, and propose circWNK1 as a promising diagnostic biomarker and therapeutic target for GC patients.

AUTHOR CONTRIBUTIONS

Ting Dai: Investigation; writing – original draft. **Shengkui Qiu:** Formal analysis; funding acquisition; investigation; writing – review and editing. **Xuesong Gao:** Data curation; funding acquisition; software. **Chengjin Zhao:** Software; validation. **Zhenming Ge:** Methodology. **Yanmei Yang:** Supervision; validation. **Chong Tang:** Conceptualization; funding acquisition; project administration. **Shichun Feng:** Conceptualization; funding acquisition; project administration; supervision.

ACKNOWLEDGMENTS

The authors would like to thank the Clinical Experimental Center of Nantong First People's Hospital for providing the experimental equipment and assistance in exploratory sample testing.

FUNDING INFORMATION

This work was supported by the Youth Program of the National Natural Science Foundation of China (82303463), the Medical Research Projects of Jiangsu Provincial Health Commission (H2019049, Z2020079), the Science and Technology Projects of Nantong City (MS2021032, MS22022003, JC2020057), the Medical Research Projects of Nantong City Health Commission (MS2022018, MB2021020), and the Kangda College of Nanjing Medical University Scientific Research Development Fund (No. KD2021KYJJZD085).

CONFLICT OF INTEREST STATEMENT

The authors declare no conflict of interest.

DATA AVAILABILITY STATEMENT

The article includes all data in the study, and further inquiries can be directed to the corresponding authors.

ETHICS STATEMENTS

Approval of the research protocol by an Institutional Reviewer Board: This study was approved by the Ethics Committee of Nantong First People's Hospital (2022KT256).

Informed Consent: All procedures were conducted in accordance with the guidelines outlined in the Declaration of Helsinki principles, and informed consent was signed by all participants.

Registry and Registration No. of the study/trial: N/A.

Animal Studies: All animal studies were approved by the Ethics Committee of the Experimental Animal Center of Nantong University (P20220218-011).

ORCID

Shengkui Qiu https://orcid.org/0000-0002-6018-7706
Shichun Feng https://orcid.org/0000-0002-0008-5193

REFERENCES

1. Sung H, Ferlay J, Siegel RL, et al. Global cancer statistics 2020: GLOBOCAN estimates of incidence and mortality worldwide for 36 cancers in 185 countries. *CA A Cancer J Clin*. 2021;71:209-249.
2. Thrift AP, Wenker TN, El-Serag HB. Global burden of gastric cancer: epidemiological trends, risk factors, screening and prevention. *Nat Rev Clin Oncol*. 2023;20:338-349. doi:10.1038/s41571-023-00747-0
3. Tan P, Yeoh K-G. Genetics and molecular pathogenesis of gastric adenocarcinoma. *Gastroenterology*. 2015;149:1153-1162.e3.
4. Chalfie M, Horvitz HR, Sulston JE. Mutations that lead to reiterations in the cell lineages of *C. elegans*. *Cell*. 1981;24:59-69.
5. Reinhart BJ, Slack FJ, Basson M, et al. The 21-nucleotide let-7 RNA regulates developmental timing in *Caenorhabditis elegans*. *Nature*. 2000;403:901-906.
6. Slack FJ, Chinnaiyan AM. The role of non-coding RNAs in oncology. *Cell*. 2019;179:1033-1055.
7. Wilusz JE, Sharp PA. A circuitous route to noncoding RNA. *Science*. 2013;340:440-441.
8. Vo JN, Cieslik M, Zhang Y, et al. The landscape of circular RNA in cancer. *Cell*. 2019;176:869-881.e13.
9. Tay Y, Rinn J, Pandolfi PP. The multilayered complexity of ceRNA crosstalk and competition. *Nature*. 2014;505:344-352.
10. Karreth FA, Pandolfi PP. ceRNA cross-talk in cancer: when ce-bling rivalries go awry. *Cancer Discov*. 2013;3:1113-1121.
11. Thomson DW, Dinger ME. Endogenous microRNA sponges: evidence and controversy. *Nat Rev Genet*. 2016;17:272-283.
12. Wang S, Zhang X, Li Z, et al. Circular RNA profile identifies circOSBPL10 as an oncogenic factor and prognostic marker in gastric cancer. *Oncogene*. 2019;38:6985-7001.
13. Zheng F, Wang M, Li Y, et al. CircNR3C1 inhibits proliferation of bladder cancer cells by sponging miR-27a-3p and downregulating cyclin D1 expression. *Cancer Lett*. 2019;460:139-151.
14. Qiu S, Li B, Xia Y, et al. CircTHBS1 drives gastric cancer progression by increasing INHBA mRNA expression and stability in a ceRNA- and RBP-dependent manner. *Cell Death Dis*. 2022;13:266.
15. Inman GJ. Switching TGFβ from a tumor suppressor to a tumor promoter. *Curr Opin Genet Dev*. 2011;21:93-99.
16. Sheen YY, Kim M-J, Park S-A, Park S-Y, Nam J-S. Targeting the transforming growth factor-β signaling in cancer therapy. *Biomol Ther*. 2013;21:323-331.
17. Colak S. Targeting TGF-β signaling in cancer. *Trends Cancer*. 2017;3:56-71.
18. Derynck R, Zhang Y, Feng XH. Smads: transcriptional activators of TGF-beta responses. *Cell*. 1998;95:737-740.
19. Troncone E, Marafini I, Stolfi C, Monteleone G. Transforming growth factor-β1/Smad7 in intestinal immunity, inflammation, and cancer. *Front Immunol*. 2018;9:1407.
20. Itoh S, ten Dijke P. Negative regulation of TGF-beta receptor/Smad signal transduction. *Curr Opin Cell Biol*. 2007;19:176-184.
21. Nakao A, Afrakhte M, Morén A, et al. Identification of Smad7, a TGFbeta-inducible antagonist of TGF-beta signalling. *Nature*. 1997;389:631-635.
22. Guo Y, Gao X, An S, et al. Deletion of miR-15a inhibited glioma development via targeting Smad7 and inhibiting EMT pathway. *Aging (Albany NY)*. 2021;13:24339-24348.
23. Yuan S, Zheng P, Sun X, et al. Hsa_Circ_0001860 promotes Smad7 to enhance MPA resistance in endometrial cancer via miR-520h. *Front Cell Dev Biol*. 2021;9:738189.
24. Ding H, Yao J, Xie H, et al. MicroRNA-195-5p downregulation inhibits endothelial mesenchymal transition and myocardial fibrosis in diabetic cardiomyopathy by targeting Smad7 and inhibiting transforming growth factor Beta 1-Smads-snail pathway. *Front Physiol*. 2021;12:709123.
25. Zeng Y, Du C, Xiao P, et al. Sox9-increased miR-322-5p facilitates BMP2-induced chondrogenic differentiation by targeting Smad7 in mesenchymal stem cells. *Stem Cells Int*. 2021;2021:9778207.
26. Harrow J, Frankish A, Gonzalez JM, et al. GENCODE: the reference human genome annotation for The ENCODE Project. *Genome Res*. 2012;22:1760-1774.

27. Esteller M. Non-coding RNAs in human disease. *Nat Rev Genet*. 2011;12:861-874.
28. Kristensen LS, Jakobsen T, Hager H, Kjems J. The emerging roles of circRNAs in cancer and oncology. *Nat Rev Clin Oncol*. 2022;19:188-206.
29. Enuka Y, Lauriola M, Feldman ME, Sas-Chen A, Ulitsky I, Yarden Y. Circular RNAs are long-lived and display only minimal early alterations in response to a growth factor. *Nucleic Acids Res*. 2016;44:1370-1383.
30. Rybak-Wolf A, Stottmeister C, Glažar P, et al. Circular RNAs in the mammalian brain are highly abundant, conserved, and dynamically expressed. *Mol Cell*. 2015;58:870-885.
31. Yan L, Chen YG. Circular RNAs in immune response and viral infection. *Trends Biochem Sci*. 2020;45:1022-1034.
32. Yang Q, Li Y, Wang Y, et al. The circRNA circSIAE inhibits replication of coxsackie virus B3 by targeting miR-331-3p and thousand and one amino-acid kinase 2. *Front Cell Infect Microbiol*. 2021;11:779919.
33. Liu C-X, Chen L-L. Circular RNAs: characterization, cellular roles, and applications. *Cell*. 2022;185:2016-2034.
34. Zhong Y, Du Y, Yang X, et al. Circular RNAs function as ceRNAs to regulate and control human cancer progression. *Mol Cancer*. 2018;17:79.
35. Zang J, Lu D, Xu A. The interaction of circRNAs and RNA binding proteins: an important part of circRNA maintenance and function. *J Neurosci Res*. 2020;98:87-97.
36. Zhang M, Huang N, Yang X, et al. A novel protein encoded by the circular form of the SHPRH gene suppresses glioma tumorigenesis. *Oncogene*. 2018;37:1805-1814.
37. Wang X, Chen L, Jin H, et al. Screening miRNAs for early diagnosis of colorectal cancer by small RNA deep sequencing and evaluation in a Chinese patient population. *Onco Targets Ther*. 2016;9:1159-1166.
38. Subbarayan K, Massa C, Lazaridou M-F, Ulagappan K, Seliger B. Identification of a novel miR-21-3p/TGF-β signaling-driven immune escape via the MHC class I/biglycan axis in tumor cells. *Clin Transl Med*. 2021;11:e306.
39. Gao Z, Liu H, Shi Y, Yin L, Zhu Y, Liu R. Identification of cancer stem cell molecular markers and effects of hsa-miR-21-3p on stemness in esophageal squamous cell carcinoma. *Cancers (Basel)*. 2019;11:E518.
40. Yue J, Tigyi G. MicroRNA trafficking and human cancer. *Cancer Biol Ther*. 2006;5:573-578.
41. Krol J, Loedige I, Filipowicz W. The widespread regulation of microRNA biogenesis, function and decay. *Nat Rev Genet*. 2010;11:597-610.
42. Gough NR, Xiang X, Mishra L. TGF-β signaling in liver, pancreas, and gastrointestinal diseases and cancer. *Gastroenterology*. 2021;161:434-452.e15.
43. Lee JH, Massagué J. TGF-β in developmental and fibrogenic EMTs. *Semin Cancer Biol*. 2022;86:136-145.
44. Derynck R, Budi EH. Specificity, versatility, and control of TGF-β family signaling. *Sci Signal*. 2019;12:eaav5183.
45. Yu Y, Feng X-H. TGF-β signaling in cell fate control and cancer. *Curr Opin Cell Biol*. 2019;61:56-63.

SUPPORTING INFORMATION

Additional supporting information can be found online in the Supporting Information section at the end of this article.

How to cite this article: Dai T, Qiu S, Gao X, et al. Circular RNA circWNK1 inhibits the progression of gastric cancer via regulating the miR-21-3p/SMAD7 axis. *Cancer Sci*. 2024;115:974-988. doi:10.1111/cas.16067